Applied Catalysis B: Environmental 91 (2009) 434–440

Contents lists available at ScienceDirect

Applied Catalysis B: Environmental

journal homepage: www.elsevier.com/locate/apcatb

Reductive dechlorination of carbon tetrachloride by zero-valent iron and related iron corrosion

Yongli Jiao [a], Cuicui Qiu [b], Lihui Huang [c], Kuixia Wu [c], Houyi Ma [b,*], Shenhao Chen [b], Luming Ma [a], Deli Wu [a,*]

[a] School of Environmental Science and Engineering, State Key Laboratory of Pollution Control and Resources Reuse, Tongji University, Shanghai 200092, China
[b] School of Chemistry and Chemical Engineering, Shandong University, Jinan 250100, China
[c] College of Environmental Science and Engineering, Shandong University, Jinan 250100, China

ARTICLE INFO

Article history:
Received 23 November 2008
Received in revised form 18 June 2009
Accepted 18 June 2009
Available online 24 June 2009

Keywords:
Dechlorination
Carbon tetrachloride (CT)
Adsorbed hydrogen
Iron
Corrosion
Hydrogen evolution

ABSTRACT

Electrochemical corrosion behavior of iron in aqueous solutions with and without carbon tetrachloride (CT) was investigated in a wide pH range from 0.4 to 14 using steady-state polarization curves and electrochemical impedance spectroscopy (EIS). It was found that the presence of CT significantly accelerated the hydrogen evolution reaction (HER) on the iron surface in strong acidic solutions, causing severe corrosion of iron; in return, the iron corrosion was helpful for the reductive dechlorination of CT. The inherent relationship between the dechlorination of CT and the corrosion of iron is attributed to the fact that the adsorbed hydrogen atoms produced during the iron corrosion process are necessary for the dechlorination process of CT. As a result, the removal efficiency of CT is strongly dependent on the extent of iron corrosion in aqueous solutions at different pH values.

1. Introduction

Carbon tetrachloride (CT), one of the commonly used chlorinated hydrocarbons, is a toxic pollutant to human health and environment [1,2]. It is reported that CT is not only a suspected human carcinogen but also an ozone depleting substance [3,4]. CT is formerly widely used in extinguisher and refrigeration, but largely abandoned now due to the toxicity. However, this substance is still used as a raw material in many industrial applications or as an industrial solvent at the present time. As a result, it is often found in groundwater or in public water systems [5,6]. In order to eliminate the threat of CT and other chlorinated hydrocarbons to both human health and environment, much effort has been devoted to the development of low-cost, high-efficiency dechlorination methods.

Reductive dechlorination of chlorinated hydrocarbons with zero-valent iron (Fe^0, ZVI) has received increasing attention in recent years since metallic iron was utilized for in situ passive groundwater remediation [7–9]. For example, permeable reactive barriers (PRBs) containing zero-valent iron have been used as an innovative method to remove chlorinated hydrocarbons in groundwater [10–13]. When wastewater passes through the barrier, the chlorinated hydrocarbons in the water will be reduced by the iron [14]. In contrast to other wastewater treatment methods, such as activated carbon adsorption, air stripping and biotransformation process, some distinct advantages of the reductive dechlorination by ZVI include mild reaction conditions, rapid reaction rate, low apparatus cost, and especially the green process technology that does not need additional chemical additives [6,15,16].

The reduction of chlorinated hydrocarbons by ZVI is essentially a surface-mediated, electrocatalytic reaction, which involves oxidation of iron, dissociation of water and reductive dechlorination of organic compounds. The possible dechlorination pathways include: (i) direct electron transfer from iron to chlorinated hydrocarbons; (ii) reduction with ferrous iron; and (iii) electrocatalytic reduction with hydrogen [2,17]. So far there has been a lot of controversy about the dechlorination mechanism of chlorinated hydrocarbons with ZVI. Because the rate of the second reaction pathway (i.e. the direct reaction between chlorinated hydrocarbons and ferrous iron produced by the iron corrosion) is quite slow, most researchers are inclined to accept that the reductive dechlorination of chlorinated hydrocarbons proceeds via the first or the third pathway [1,18]. Some authors believe the chlorinated hydrocarbons are mainly degraded through the direct reaction of chlorinated hydrocarbons with

* Corresponding authors. Fax: +86 531 88564464.
E-mail addresses: hyma@sdu.edu.cn (H. Ma), wudeli@tongji.edu.cn (D. Wu).

0926-3373/$ – see front matter © 2009 Elsevier B.V. All rights reserved.
doi:10.1016/j.apcatb.2009.06.012

Fe^0 (ZVI) at the iron surface [7,18]. However, the viewpoint contradicts with the experimental results that the rate of reductive dehalogenation of halohydrocarbons is correlated to the pH or hydrogen ion concentration [8,18–22]. No matter whether chlorinated hydrocarbons are dechlorinated through the direct reduction by Fe^0 or through the indirect reduction by hydrogen species, the iron will suffer more severe corrosion unavoidably in the solutions containing chlorinated hydrocarbons. In this sense, there exists inherent relation between the corrosion of iron and the dechlorination of chlorinated hydrocarbons although there have been few studies in this aspect [22]. It is possible to give an in-depth understanding of electrochemical reductive dechlorination of chlorinated hydrocarbons by studying the corrosion behavior of iron in the presence of chlorinated hydrocarbons.

In this paper, we studied the corrosion of iron in the presence of CT and the electrochemical reductive dechlorination of CT at the iron electrode in solutions with different pH values to explore the link between the two reaction processes. The obtained results clearly indicate that the dechlorination of CT is coupled with the hydrogen evolution reaction (HER) at the iron surface. This new finding is of fundamental importance to better understand the reductive dechlorination mechanism of chlorinated organic compounds by ZVI.

2. Experimental

A 2.0 mm-diameter iron rod (Aldrich 99.999%) was employed to prepare the working electrode. The iron rod specimen was embedded in epoxy resin mould, leaving its cross-section only exposed to the electrolyte solutions. Before use, the iron electrode was polished with emery papers of decreasing particle size to #2000 finish at first, then rinsed with ultrapure water and degreased with acetone.

The chemicals used in the experiments, carbon tetrachloride (CT), sulfuric acid, sodium sulfate and sodium hydroxide, were of AR grade and were used as received. All of the aqueous solutions were prepared with ultrapure water (>18 MΩ cm). Electrochemical reductive dechlorination of CT was carried out in H_2SO_4, Na_2SO_4 and the mixed solutions of H_2SO_4 + Na_2SO_4 or Na_2SO_4 + NaOH with different pH values, respectively.

Steady-state polarization curves and EIS measurements were performed with a CHI 760C and a Zahner IM6 electrochemical workstation, respectively in a conventional three-electrode cell at room temperature (~25 °C). A bright Pt plate (1.0 cm × 2.0 cm) served as the counter electrode, and a saturated calomel electrode (SCE) was selected as the reference electrode. The reference electrode was led to the surface of the working electrode through a Luggin capillary. As for the impedance measurements, applying a sinusoidal wave of ±5 mV amplitude at the designated potentials, all impedance sweeps used 10 frequencies per decade within the frequency range from 60 kHz to 10 mHz. The electrolyte solutions were deaerated by N_2 bubbling for 10 min before addition of CT, and a blanket of N_2 was maintained throughout each experiment.

The concentration of CT in the electrolytes before and after potentiostatic electrolysis was analyzed by gas chromatography/mass spectrometry (GC/MS)-QP2010. The GC was equipped with a DB-5 MS capillary column (30 m × 0.25 mm, 0.25 μm thickness). The column temperature was 35 °C, injection port temperature was 200 °C, and the ion-trap detector temperature was 200 °C. Ultrapure He was used as the carrier gas at a flow rate of 1.1 mL min^{-1} and a split ratio of 60:1. The carbon tetrachloride removal rate was determined by comparing the concentration of CT in the solutions before and after electrochemical reductive dechlorination.

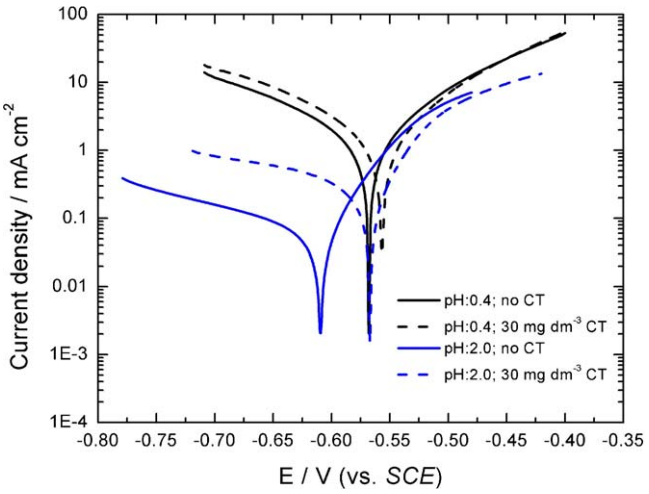

Fig. 1. Steady-state polarization curves for an iron electrode in 0.5 mol dm^{-3} H_2SO_4 solutions (pH 0.4) and H_2SO_4–Na_2SO_4 mixed solutions (pH 2.0) with and without carbon tetrachloride (CT).

3. Results and discussion

3.1. Influence of CT on the corrosion behavior of iron in acidic solutions

Fig. 1 shows a set of steady-state polarization curves for the iron electrode in strong acid solutions with and without CT. In the solution with low pH (pH 0.4), the cathodic current was obviously enhanced by CT, while the anodic current was almost not affected by the presence of CT. Interestingly, CT did not cause any obvious change in cathodic Tafel slope, and two cathodic polarization curves gave the almost identical slope of ~120 mV $decade^{-1}$ between −0.59 and −0.67 V, which implies the rate-determining step (rds) of hydrogen evolution reaction (HER) remained unchanged although the rate of the HER was strongly accelerated by CT. In contrast, in the solution with high pH (pH 2), the corrosion rates of iron in the presence and absence of CT both decreased significantly, which is exemplified by the obvious decrease in corrosion current densities. Despite all this, the comparison of two polarization curves clearly indicates that the presence of CT aggravated the iron corrosion to a greater degree in the latter case.

The reduction of halogenated organic compounds by Fe^0 is a heterogeneous electrochemical reaction involving the oxidation of iron and the reduction of halogenated compound [19]. In the presence of proton donors, the direct reaction of Fe^0 with alkyl halides (written as R–X),

$$Fe^0 + R{-}X + H^+ \rightarrow Fe^{2+} + R{-}H + X^- \quad (1)$$

is a thermodynamically favorable reaction under most conditions, which is essentially equivalent to iron corrosion with the alkyl halide serving as the oxidizing agent [8]. For the present Fe–CCl_4–H_2SO_4 system, with the exception of Fe^0, there were still other reducing agents, such as Fe^{2+} ions and H_2 which were produced from the corrosion of the iron electrode in acidic solutions [23]. According to Matheson and Tratnyek [8], the reduction of CT with Fe^0 should include direct reduction by Fe^0 and indirect reduction with Fe^{2+} ions and H_2. The indirect reduction by H_2 is usually fast with low hydrogen overpotential metals such as Pt or Pd, but relatively slow at high hydrogen overpotential ones such as Fe [8,19,22]. Atomic hydrogen is a very powerful reducing agent that can degrade chlorinated hydrocarbons through a surface-mediated process, therefore many researchers incorporate a second metal, such as Pd, into ZVI (Fe^0) so that the atomic hydrogen produced

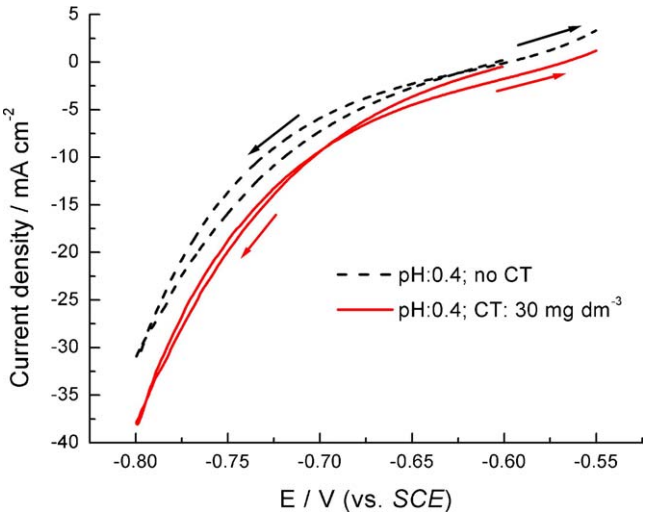

Fig. 2. Voltammetric curves for hydrogen evolution at the iron surface in 0.5 mol dm^{-3} H_2SO_4 solutions (pH 0.4) with and without CT. Scan rate: 20 mV s^{-1}.

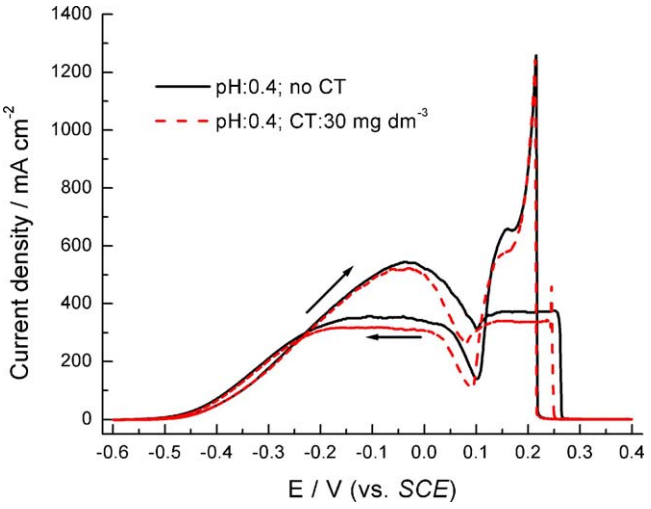

Fig. 3. . Cyclic voltammograms (CVs) describing the anodic behavior of iron in CT-free and CT-containing 0.5 mol dm^{-3} H_2SO_4 solutions (pH 0.4). Scan rate: 20 mV s^{-1}.

from the iron corrosion evolves more easily at the Pd surface [2,22]. However, in the case of high hydrogen ion concentration, especially when the reduction of R–X is coupled with the HER, the contribution of adsorbed hydrogen atoms on the iron to the R–X degradation cannot be ignored [24]. The great enhancement effect of CT on the cathodic reaction shown in Fig. 1 is probably associated with a dechlorination reaction dependent on the hydrogen atoms (e.g. $CCl_4 + H + e^- \rightarrow CHCl_3 + Cl^-$), which drives the overall process [25].

Now that CT may be reduced indirectly via reaction with atomic hydrogen adsorbed on the iron surface, the corrosion of iron in the acidic solutions containing CT should be the hydrogen evolutional corrosion related to reductive dechlorination of CT. It is possible to have better insight into the reductive dechlorination mechanism of CT by studying the corrosion behavior of iron in acidic solutions. Fig. 2 shows the voltammograms for the HER at the iron surface in the wider cathodic potentials in CT-free and CT-containing 0.5 mol dm^{-3} H_2SO_4 solutions. It was found by comparing two CV curves that the HER was promoted by the CT in the whole potential range investigated. At the same time, obvious gas evolution was observed to occur at ~−0.65 V in the presence of CT, about 35 mV more positive than that in the absence of CT. It is obvious that the presence of tiny amount of CT strongly accelerated the HER on the iron surface, leading to the severe corrosion of iron in the CT-containing solutions.

Theoretically, there is a probability that the ferrous ions produced during the iron corrosion can be further oxidized to ferric ions, coupled with reduction of CT [5].

$$2Fe^{2+} + CCl_4 + H^+ \rightarrow 2Fe^{3+} + CHCl_3 + Cl^- \quad (2)$$

However, because the ferrous ion concentration is too low in the corrosion media, the reductive dechlorination of CT via the pathway shown by Eq. (2) is negligible. In fact, Fig. 1 has demonstrated that CT has only a slight influence on the anodic dissolution of iron in strong contrast to its accelerating effect on the HER, from which it is inferred that ferrous iron species on the iron electrode formed during anodic dissolution of iron hardly affected the reduction of CT. If so, the reductive dechlorination of CT with Fe^0 should be more closely associated with the hydrogen atoms producing from the HER. In order to confirm the inference, we investigated the anodic polarization behavior of iron in a wide range of anodic potentials in H_2SO_4 solutions with and without CT. The cyclic voltammograms (CVs) of the iron electrode measured in two solutions are shown in Fig. 3. The two CV curves are very similar in shape, peak potentials and current magnitude and exhibit typical voltammetric characteristics of the iron [26], including active dissolution region, prepassive one, oscillatory one and passivation one. It is concluded that the CT hardly affects the anodic polarization behavior of the iron by comparing the two CVs shown in Fig. 3. Although this result cannot completely exclude the possibility that CT reacts with ferrous iron, we are sure that reduction of CT by the ferrous iron is insignificant during the dechlorination process of CT.

3.2. Influence of CT concentration on the iron corrosion in acidic and neutral solutions studied by Tafel curves

Considering that the reductive dechlorination of chlorinated hydrocarbons with Fe^0 is usually applied under open-circuit conditions, here we focused on investigating the corrosion of iron related to the dechlorination of CT around the open-circuit potentials (OCPs). Fig. 4 describes the influence of CT concentration on the corrosion behavior of iron in acidic solutions. When the CT concentration was very low (1.6 mg dm^{-3}), CT had little influence

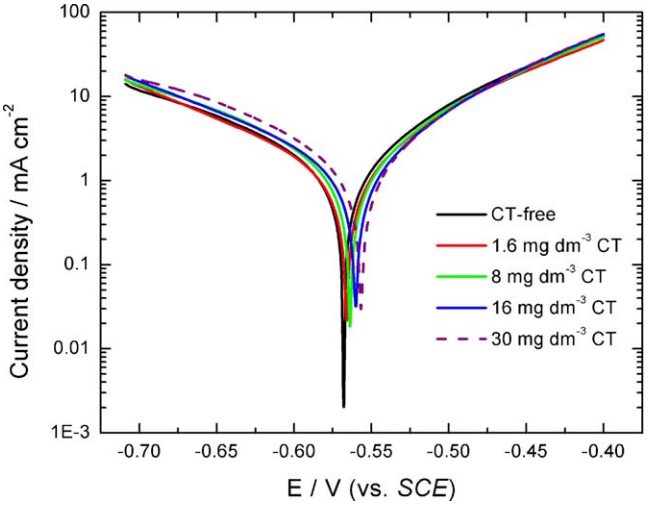

Fig. 4. Steady-state polarization curves for the iron electrode in CT-free and CT-containing 0.5 mol dm^{-3} H_2SO_4 solutions (pH 0.4). The concentrations of CT in 0.5 mol dm^{-3} H_2SO_4 solutions are 1.6, 8.0, 16 and 30 mg dm^{-3}, respectively.

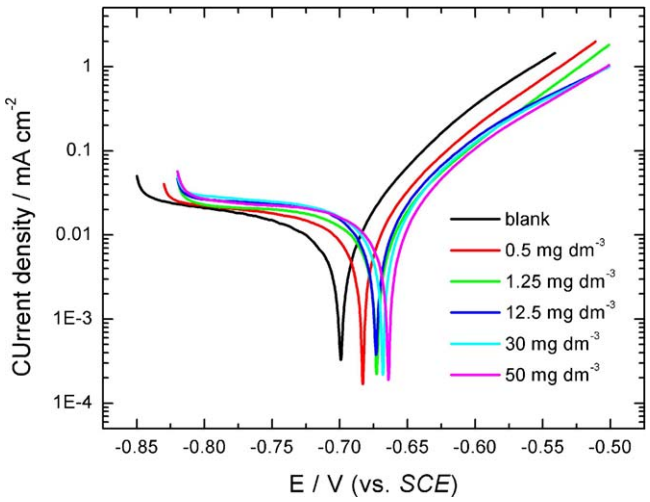

Fig. 5. Steady-state polarization curves for the iron electrode in CT-free and CT-containing 0.05 mol dm^{-3} Na_2SO_4 solutions (pH 7.0). The concentrations of CT in Na_2SO_4 solutions are 0.5, 1.25, 12.5, 30 and 50 mg dm^{-3}, respectively.

on the cathodic polarization (i.e. HER) but slightly inhibited the anodic iron dissolution. With the increase of CT concentration, the HER tended to be accelerated strongly. The higher the CT concentration, the larger the cathodic current for the HER. In contrast, the iron dissolution was inhibited at low polarization potentials but was almost not affected from −0.47 V to more positive potentials. Obviously, the corrosion of iron is strongly dependent on the CT concentration, more exactly, the strong acceleration role of CT to the HER.

Seeing that the Fe^0 is applied more widely to electrochemical dechlorination of chlorinated hydrocarbons in neutral water environment, we also investigated the corrosion behavior of iron in neutral Na_2SO_4 solutions with different CT concentrations. The obtained results are shown in Fig. 5. For iron corroding in CT-free Na_2SO_4 solutions, the over corrosion reaction consists of the anodic dissolution of iron and the cathodic reduction of dissolved oxygen. As indicated by the black line, the cathodic polarization curve of iron measured in the neutral solutions, quite different from that obtained in acidic solutions, displayed a current plateau from −0.75 to −0.84 V, which is attributed to the diffusion-controlled reduction of the oxygen at the electrode/solution interface. In the presence of CT, the corrosion behavior of iron did not change significantly except the corrosion potential was shifted towards more positive values with increasing CT concentrations. It is clear that CT has a slight influence on the iron corrosion under neutral conditions. This further demonstrates from another side that CT strongly accelerates the iron corrosion under acidic conditions through enhancing the rate of HER.

3.3. EIS study of the iron corrosion in strong acidic solutions with CT

Electrochemical impedance spectroscopy (EIS) is a powerful method for analyzing reaction mechanisms of metal corrosion involving adsorbed intermediates and for elucidating the change of the surface states of electrodes [26,27]. The steady-state polarization curves shown in Figs. 1 and 4 have demonstrated that the serious corrosion of iron in the CT-containing solutions arose from the acceleration role of CT to the HER. We want to further know whether CT molecules participate in the HER and form adsorbed intermediate species on the iron surface. EIS is very helpful for giving a clear presentation of the corrosion process of iron related to the dechlorination of CT.

Fig. 6 presents EIS spectra for the iron in 0.5 mol dm^{-3} H_2SO_4 solutions with and without CT at the potentials 15 mV more

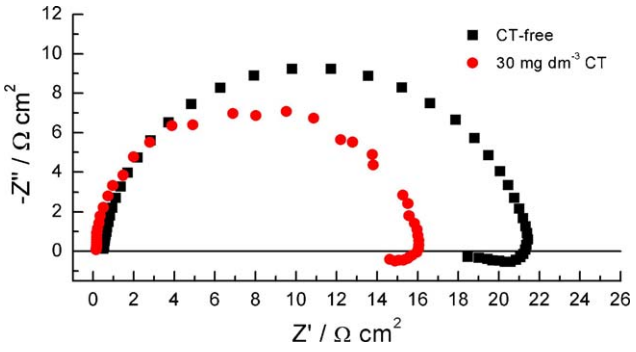

Fig. 6. Nyquist impedance spectra for the iron electrode in 0.5 mol dm^{-3} H_2SO_4 solutions (pH 0.4) with and without CT.

negative than their respective OCPs. The two spectra are similar in profile with difference in size and both give a high frequency semicircle (more exactly capacitive loop) and a low frequency inductive loop. The high frequency capacitive loop is usually related to the relaxation time constant of the charge-transfer resistance (R_t) and the double-layer capacitance (C_{dl}) at the electrode/solution interface, and the low frequency inductive loop is attributed to the relaxation time constant of adsorbed species [27,28]. The similarity of two EIS spectra implies that the corrosion mechanism of iron in both cases is basically the same.

The capacitive loops of the aforementioned two EIS spectra can be fitted well with the equivalent circuit shown in Fig. 7. In this circuit, R_s is the solution resistance between the iron electrode and the reference electrode, R_t is the charge-transfer resistance, and Q_{dl} represents the constant phase element (CPE) modeling the double-layer capacitance (C_{dl}). Admittance and impedance of a CPE are, respectively, defined as [28–30]:

$$Y_Q = Y_0(j\omega)^n \tag{3}$$

and

$$Z_Q = \frac{1}{Y_0}(j\omega)^{-n} \tag{4}$$

where subscript Q denotes a CPE, Y_0 is the modulus, ω is the angular frequency, and n is the phase. The values of elements of the circuit obtained by fitting the two EIS spectra were given in Table 1. The values of the double-layer capacitance were calculated by means of our previously proposed method [28,30] and are also listed in this table.

Values of R_t can be used to evaluate the degree of corrosion. The smaller the R_t, the more serious the iron corrosion. It is determined that the iron suffered more severe corrosion in the presence of CT than in the absence of CT based on the values of R_t (20.3 Ω cm^2 in CT-free solution and 15.3 Ω cm^2 in CT-containing solution). In addition, we noticed that there was not obvious difference between the values of C_{dl} obtained in two cases. This excludes the possibility of strong adsorption of CT molecules on the iron surface around the OCPs.

In view of strong accelerating effect of CT on the HER, the impedance behavior of iron at different cathodic polarization potentials was investigated in H_2SO_4 solutions with and without

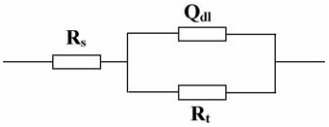

Fig. 7. An equivalent circuit that describes the high frequency capacitive loop associated with the relaxation process of the charge-transfer resistance and the double-layer capacitance.

Table 1
Values of elements of the equivalent circuit in Fig. 7 obtained by fitting the high frequency capacitive loops shown in Figs. 6 and 9, and calculated values of C_{dl}.

	R_s (Ω cm^2)	$Q_{dl}Y_0$ (Ω^{-1} cm^{-2} s^n, n/0–1)	C_{dl} (μF cm^{-2})	R_t (Ω cm^2)
0.5 mol dm^{-3} H_2SO_4 (pH 0.4)	4.87×10^{-1}	Y_0: 6.02×10^{-5}; n: 9.34×10^{-1}	3.75×10^{1}	2.03×10^{1}
0.5 mol dm^{-3} H_2SO_4 + 30 mol dm^{-3} CT (pH 0.4)	1.45×10^{-1}	Y_0: 5.0×10^{-5}; n: 9.82×10^{-1}	4.38×10^{1}	1.53×10^{1}
0.05 mol dm^{-3} Na_2SO_4 (pH 7)	1.71	Y_0: 1.64×10^{-3}; n: 8.17×10^{-1}	1.96×10^{3}	1.36×10^{3}
0.05 mol dm^{-3} Na_2SO_4 + 0.5 mol dm^{-3} CT (pH 7)	1.54	Y_0: 9.43×10^{-4}; n: 7.93×10^{-1}	1.01×10^{3}	1.38×10^{3}
0.05 mol dm^{-3} Na_2SO_4 + 1.25 mol dm^{-3} CT (pH 7)	1.58	Y_0: 7.33×10^{-4}; n: 8.11×10^{-1}	6.94×10^{2}	1.08×10^{3}
0.05 mol dm^{-3} Na_2SO_4 + 12.5 mol dm^{-3} CT (pH 7)	1.56	Y_0: 8.76×10^{-4}; n: 8.11×10^{-1}	8.78×10^{2}	1.15×10^{3}
0.05 mol dm^{-3} Na_2SO_4 + 30 mol dm^{-3} CT (pH 7)	1.64	Y_0: 9.30×10^{-4}; n: 8.07×10^{-1}	9.29×10^{2}	1.07×10^{3}
0.05 mol dm^{-3} Na_2SO_4 + 50 mol dm^{-3} CT (pH 7)	1.61	Y_0: 8.62×10^{-4}; n: 8.19×10^{-1}	8.45×10^{2}	1.06×10^{3}

CT. Fig. 8 shows that, at the same cathodic potentials, the impedance spectra measured in the CT-free and CT-containing solutions are similar in profile with difference in size; and moreover, the changes in both shape and size of impedance spectra with the applied cathodic potentials in the presence of CT have the same trend as that in the absence of CT. The more negative the applied potential, the smaller the diameter of high frequency capacitive loop, implying that the rate of HER becomes fast with increasing cathodic potential. If comparing the EIS spectra measured at the identical polarization potentials in the two solutions, it is not difficult to draw such a conclusion that the presence of CT really accelerates the rate of the HER but does not alter the mechanism of the HER.

HER is a two-step reaction, which is described as follows [31]:

$$M + H^+ + e^- \overset{\text{discharge}}{\longrightarrow} MH_{ads} \quad (5)$$

where M denotes a metal, and MH_{ads} represents an H atom adsorbed on an M atom which formed after a proton discharged onto the active surface sites of M, followed by

$$2\,MH_{ads} \overset{\text{catalysis}}{\longrightarrow} H_2 + M \quad (6)$$

or

$$H^+ + MH_{ads} + e^- \overset{\text{discharge}}{\longrightarrow} H_2 + M \quad (7)$$

Based on the cathodic Tafel slope of ~120 mV decade^{-1} shown in Figs. 1 and 4 and appearance of inductive loops at low cathodic potentials observed in Figs. 6 and 8, herein we assumed that the HER proceeded via a reaction pathway consisting of Eqs. (5) and (7), in which Eq. (5) was the rate-determining steps (rds) and Eq. (7) was a fast step. In this pathway, the desorption reaction consists of second discharge reaction of protons on top of the adsorbed H atoms produced via Eq. (5) [31]. In the presence of chlorinated hydrocarbons (written as R–Cl), it is possible that adsorbed H atoms may diffuse across the electrode surface and react with R–Cl molecules to form R–H through Eq. (8),

$$MH_{ads} + R - Cl \overset{\text{catalysis}}{\longrightarrow} R - H + M - Cl \quad (8)$$

leading to the reductive dechlorination of R–Cl. In this way, the dechlorination reaction of CT should be a competitive reaction, coupling with the electrochemical desorption of H atoms. The role of CT is indirectly promoting the rate of rds through partially consuming the adsorbed H atoms on the iron surface, but does not directly participate in the rds (Eq. (5)).

According to this mechanism for reductive dechlorination of R–Cl, the effect of CT on the HER is related to its concentration. The CT should have a slight influence on the HER when its concentration is very low (e.g. 1.6 mg dm^{-3}). In this case electrochemical desorption reaction (Eq. (7)) dominates over the chemical desorption step (Eq. (8)) in the competition. CT begins to play an important role in enhancing the rate of HER with the concentration increase of CT, as indicated by Fig. 4. Because Eq. (8) is a potential-independent reaction, the presence of CT will not bring about marked changes to impedance behavior of the iron. This is probably the reason why the impedance spectra of the iron electrode in the presence of CT are similar to those obtained in the absence of CT.

3.4. Influence of pH on removal efficiency of CT

As mentioned above, the dechlorination process of CT at the iron electrode in acidic solutions should be considered as a special electrocatalytic hydrogenolysis (ECH), which strongly accelerates the cathodic evolution of hydrogen on the iron surface, causing the severe corrosion of iron. Because this process is sensitive to pH changes, it is expected that the acceleration effect of CT on the HER will decrease with the rising of pH value. The inference has been supported by the steady-state polarization curves shown in Fig. 5 and further confirmed by EIS results of iron electrodes in the neutral Na_2SO_4 solutions containing different concentrations of CT. Fig. 9 exhibits a group of Nyquist impedance spectra for the iron at the OCPs in the blank solutions and in the presence of various

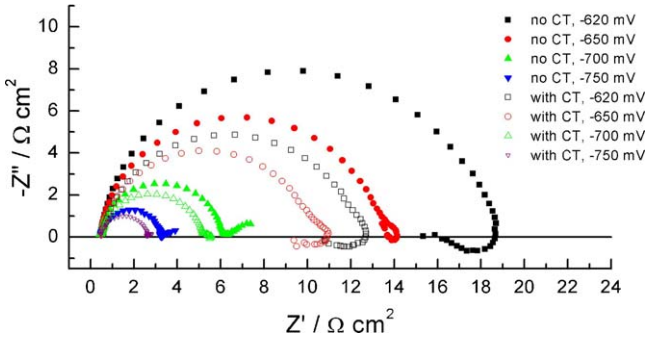

Fig. 8. A set of Nyquist impedance spectra for the iron electrode measured at different cathodic polarization potentials in 0.5 mol dm^{-3} H_2SO_4 solutions (pH 0.4) with and without CT (30 mg).

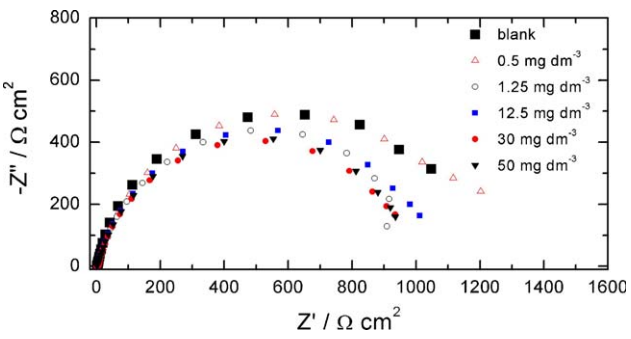

Fig. 9. A set of Nyquist impedance spectra for the iron electrode measured at their open-circuit potentials (OCPs) in 0.05 mol dm^{-3} Na_2SO_4 solutions (pH 7.0) with and without CT.

Table 2
The efficiency for reductive dechlorination of carbon tetrachloride (CT) at different potentials on the iron electrode in aqueous solutions of different pH values.

Solutions	Experimental conditions	Removal efficiency of CT/%
0.5 mol dm^{-3} H_2SO_4 + 30 mg dm^{-3} CT (pH 0.4)	Without dechlorination	–
0.5 mol dm^{-3} H_2SO_4 + 30 mg dm^{-3} CT (pH 0.4)	At −0.62 V for 30 min	79.2
0.5 mol dm^{-3} H_2SO_4 + 30 mg dm^{-3} CT (pH 0.4)	At −0.56 V for 30 min (20 mV more negative than the OCP)	28.9
H_2SO_4–Na_2SO_4 + 30 mg dm^{-3} CT (pH 2)	At −0.62 for 30 min	56.6
H_2SO_4–Na_2SO_4 + 30 mg dm^{-3} CT (pH 2)	At −0.59 V for 30 min (20 mV more negative than the OCP)	22.5
0.05 mol dm^{-3} Na_2SO_4 + 30 mg dm^{-3} CT (pH 7)	At OCP for 30 min (E_{ocp} = −0.67 V)	2.55
0.05 mol dm^{-3} Na_2SO_4 + 30 mg dm^{-3} CT (pH 7)	At −0.69 V for 30 min (20 mV more negative than the OCP)	7.25
Na_2SO_4–NaOH + 30 mg dm^{-3} CT (pH 12)	At OCP for 30 min (E_{ocp} = −0.67 V)	2.49
Na_2SO_4–NaOH + 30 mg dm^{-3} CT (pH 12)	At −0.69 V for 30 min (20 mV more negative than the OCP)	4.83

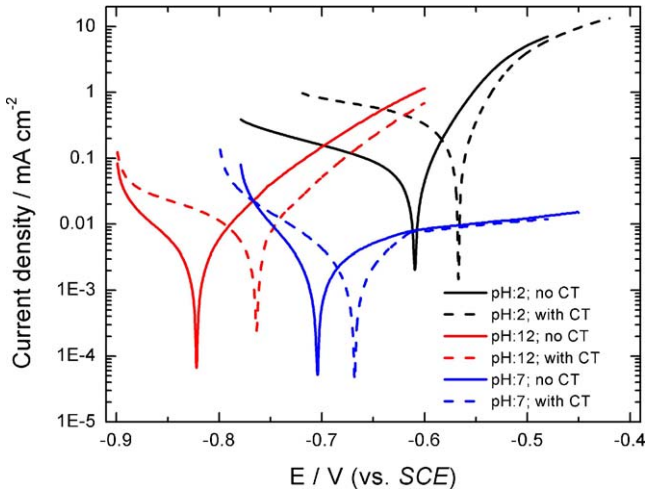

Fig. 10. A group of steady-state polarization curves for the iron electrode measured in CT-free and CT-containing H_2SO_4–Na_2SO_4 mixed solutions (pH 2.0), 0.05 mol dm^{-3} Na_2SO_4 solutions (pH 7.0) and Na_2SO_4–NaOH mixed solutions (pH 12), respectively.

concentrations of CT. All these impedance spectra display incomplete capacitive loops with relatively large diameters (>1000 Ω cm^2). They were fitted using the equivalent circuit in Fig. 7, and the obtained element values were listed in Table 1. In neutral aqueous solutions, CT had little influence on the iron corrosion when its concentration was very low (0.5 mg dm^{-3}), which is exemplified in the almost identical capacitive loops in size in the solutions with and without CT. Even though the CT concentration increased from 1.25 to 50 mg dm^{-3}, the diameter of capacitive loops only slightly decreased from 1.08×10^3 to 1.06×10^3 Ω cm^2. Because CT hardly affects the cathodic reduction of oxygen at the iron surface, there is not too obvious change in the corrosion rate of iron before and after the addition of CT.

Fig. 10 shows a set of steady-state polarization curves for the iron electrode measured in aqueous solutions with different pH values in the presence and absence of CT. It is observed from that the rate of iron corrosion decreased with increasing pH values, regardless of whether or not there existed CT. In contrast with the significant influence of CT on the iron corrosion in strong acidic solutions, the presence of CT altered the cathodic Tafel slope in neutral (pH 7.0) and alkaline (pH 12) solutions. The main reason is that the cathodic reaction was no longer the HER and became the electrochemical reduction of oxygen. The adsorption of CT molecules on the iron hampered the charge-transfer from the electrode/solution interface to the oxygen species and the diffusion of oxygen dissolved in the electrolytes from the bulk solution to the electrode surface. This effect seemed particularly obvious in the alkaline solution. The cathodic current increased slowly with the polarization potential in the potential region between −0.81 and −0.87 V, forming a current plateau.

According to Eqs. (5)–(8), the dechlorination reaction of CT is coupled with the HER at the iron surface. Theoretically, low pH values should favor the dechlorination of CT. In order to investigate the influence of pH value and applied cathodic potential on the CT dechlorination, electrochemical reductive dechlorination of CT at the iron surface was performed in potentiostatic mode in aqueous solutions with different pH values. The removal efficiencies of CT obtained under different conditions are shown in Table 2. As expected, in acidic solutions, the lower the pH value and the more negative the applied potential, the higher the removal efficiency of CT. For example, the removal efficiency of CT in 0.5 mol dm^{-3} H_2SO_4 solution (pH 0.4) at −0.62 V reached 79.2%. On the contrary, in neutral and alkaline solutions, the removal efficiency values of CT at the respective OCPs or at cathodic potentials were all relatively low (<10%). In this situation, the influence of pH on the CT dechlorination was insignificant. Thus, we can conclude that, although Fe^0 may directly react with the CT molecules, resulting in the dechlorination of small amount of CT, the adsorbed hydrogen atoms on the iron surface play the more important role in reductive dechlorination of CT. The low pH value is advantageous to the dechlorination of CT, without question.

4. Conclusions

The reductive dechlorination of CT with ZVI (Fe^0) is essentially a catalytic reaction between CT molecules and the adsorbed hydrogen atoms. Because this reaction is a parallel, competitive reaction that is coupled with electrochemical desorption reaction of adsorbed hydrogen atoms, the presence of CT significantly accelerates the rate of the HER in acidic solutions, especially in the strong acidic solutions, thereby causing the more serious corrosion of iron than in blank solutions. Consequently, there exists inherent relationship between the dechlorination of CT and the corrosion of iron. The lower the pH value of the electrolyte, the faster the dechlorination reaction of CT proceeds; and in turn the higher the dechlorination efficiency of CT, the more severe the iron corrosion.

Acknowledgments

This work was supported by the National 973 Program Projects of China (2006CB605004, 2007CB936602), the National Natural Science Foundation of China (20673067) and China High-tech Research and Development Plan (2008AA06Z310).

References

[1] R.A. Maithreepala, R.-A. Doong, Environ. Sci. Technol. 38 (2004) 6676–6684.
[2] H.-L. Lien, W.-X. Zhang, Appl. Catal. B: Environ. 77 (2007) 110–116.
[3] M. Ogeturk, I. Kus, N. Colakoglu, I. Zararsiz, N. Ilhan, M. Sarsilmaz, J. Ethnopharmacol. 97 (2005) 273–280.
[4] R.E. Doherty, Environ. Forensics 1 (2000) 69–81.
[5] B.R. Helland, P.J.J. Alvarez, J.L. Schnoor, J. Hazard. Mater. 41 (1995) 205–216.
[6] V. Janda, P. Vasek, J. Bizova, Z. Belohlav, Chemosphere 54 (2004) 917–925.
[7] T. Li, J. Farrell, Environ. Sci. Technol. 34 (2000) 173–179.
[8] L.J. Matheson, P.G. Tratnyek, Environ. Sci. Technol. 28 (1994) 2045–2053.

[9] J.L. Chen, S.R. Al-Abed, J.A. Ryan, Z.B. Li, J. Hazard. Mater. 83 (2001) 243–254.
[10] R. Thiruverikatachari, S. Vigneswaran, R. Naidu, J. Ind. Eng. Chem. 14 (2008) 145–156.
[11] R.T. Wilkin, R.W. Puls, G.W. Sewell, Ground Water 41 (2003) 493–503.
[12] R.W. Puls, D.W. Blowes, R.W. Gillham, J. Hazard. Mater. 68 (1999) 109–124.
[13] R.A. Maithreepala, R.A. Doong, Environ. Sci. Technol. 39 (2005) 4082–4090.
[14] B.A. Logue, J.C. Westall, Environ. Sci. Technol. 37 (2003) 2356–2362.
[15] Y.X. Fang, S.R. Al-Abed, Appl. Catal. B: Environ. 78 (2008) 371–380.
[16] G. Kim, W. Jeong, S. Choe, J. Hazard. Mater. 155 (2008) 502–506.
[17] P.M.L. Bonin, M.S. Odziemkowski, R.W. Gillham, Corros. Sci. 40 (1998) 1391–1409.
[18] K.D. Warren, R.G. Arnold, T.L. Bishop, L.C. Lindholm, E.A. Betterton, J. Hazard. Mater. 41 (1995) 217–227.
[19] J. Feng, T.-T. Lim, Chemosphere 59 (2005) 1267–1277.
[20] M.M. Scherer, J.C. Westall, P.G. Tratnyek, Corros. Sci. 44 (2002) 1151–1157.
[21] P.M.L. Bonin, W. Jedral, M.S. Odziemkowski, R.W. Gillham, Corros. Sci. 42 (2000) 1921–1939.
[22] Y. Fang, S.R. Al-Abed, Environ. Sci. Technol. 42 (2008) 6942–6948.
[23] R.W. Gillham, S.F. O'Hannesin, Ground Water 32 (1994) 958–967.
[24] J. Wang, J. Farrell, Environ. Sci. Technol. 37 (2003) 3891–3896.
[25] T.L. Johnson, W. Fish, Y.A. Gorby, P.G. Tratnyek, J. Contam. Hydrol. 29 (1998) 379–398.
[26] H.Y. Ma, G.Q. Li, S.C. Chen, S.Y. Zhao, X.L. Cheng, Corros. Sci. 44 (2002) 1177–1191.
[27] H.Y. Ma, X.L. Cheng, S.H. Chen, C. Wang, J.P. Zhang, H.Q. Yang, J. Electroanal. Chem. 451 (1998) 11–17.
[28] X.J. Wu, H.Y. Ma, S.H. Chen, Z.Y. Xu, A.F. Sui, J. Electrochem. Soc. 146 (1999) 1847–1853.
[29] H.Y. Ma, L.Y. Ou Yang, N. Pan, S.L. Yau, J.Z. Jiang, K. Itaya, Langmuir 22 (2006) 2105–2111.
[30] H.Y. Ma, X.L. Cheng, G.Q. Li, S.H. Chen, Z.L. Quan, S.Y. Zhao, L. Niu, Corros. Sci. 42 (2000) 1669–1683.
[31] J.O'M. Bockris, S.U.M. Khan, Surface Electrochemistry: A Molecular Level Approach, Plenum, New York, 1993, pp. 313–316.